The Journal of Infectious Diseases

MAJOR ARTICLE

Ebola Virus Disease Features Hemophagocytic Lymphohistiocytosis/Macrophage Activation Syndrome in the Rhesus Macaque Model

David X. Liu,[1,a] Bapi Pahar,[1,a] Timothy K. Cooper,[1] Donna L. Perry,[1] Huanbin Xu,[2] Louis M. Huzella,[1] Ricky D. Adams,[1] Amanda M. W. Hischak,[1] Randy J. Hart,[1] Rebecca Bernbaum,[1] Deja Rivera,[1] Scott Anthony,[1] Marisa St Claire,[1] Russell Byrum,[1] Kurt Cooper,[1] Rebecca Reeder,[1] Jonathan Kurtz,[1] Kyra Hadley,[1] Jiro Wada,[1] Ian Crozier,[3] Gabriella Worwa,[1] Richard S. Bennett,[1] Travis Warren,[1] Michael R. Holbrook,[1] Connie S. Schmaljohn,[1] and Lisa E. Hensley[1,b]

[1]Integrated Research Facility at Fort Detrick, Division of Clinical Research, National Institute of Allergy and Infectious Diseases, National Institutes of Health, Fort Detrick, Frederick, Maryland, USA; [2]Department of Comparative Pathology, Tulane National Primate Research Center, Covington, Louisiana, USA; and [3]Clinical Monitoring Research Program Directorate, Frederick National Laboratory for Cancer Research, Frederick, Maryland, USA

Background. Ebola virus (EBOV) disease (EVD) is one of the most severe and fatal viral hemorrhagic fevers and appears to mimic many clinical and laboratory manifestations of hemophagocytic lymphohistiocytosis syndrome (HLS), also known as *macrophage activation syndrome*. However, a clear association is yet to be firmly established for effective host-targeted, immunomodulatory therapeutic approaches to improve outcomes in patients with severe EVD.

Methods. Twenty-four rhesus monkeys were exposed intramuscularly to the EBOV Kikwit isolate and euthanized at prescheduled time points or when they reached the end-stage disease criteria. Three additional monkeys were mock-exposed and used as uninfected controls.

Results. EBOV-exposed monkeys presented with clinicopathologic features of HLS, including fever, multiple organomegaly, pancytopenia, hemophagocytosis, hyperfibrinogenemia with disseminated intravascular coagulation, hypertriglyceridemia, hypercytokinemia, increased concentrations of soluble CD163 and CD25 in serum, and the loss of activated natural killer cells.

Conclusions. Our data suggest that EVD in the rhesus macaque model mimics pathophysiologic features of HLS/macrophage activation syndrome. Hence, regulating inflammation and immune function might provide an effective treatment for controlling the pathogenesis of acute EVD.

Keywords. Ebola virus disease; hemophagocytic lymphohistiocytosis syndrome; macrophage activation syndrome; sCD163; sCD25.

Hemophagocytic lymphohistiocytosis syndrome (HLS), also known as macrophage activation syndrome (MAS), is a potentially fatal condition characterized by a dysregulated hyperinflammatory response and/or increased cytokine production associated with the uncontrolled proliferation and activation of macrophages and lymphocytes [1]. HLS has been classified into 2 forms based on a genetic or acquired etiology. Primary, or familial, HLS refers to genetic mutations typically affecting perforin and intracellular vesicle formation in cytotoxic T lymphocytes and natural killer (NK) cells. Acquired HLS, or secondary HLS (sHLS), is usually associated with a wide array of nongenetic diseases, including infectious diseases [1].

Clinically, sHLS/MAS is more common in adults than in children and is usually associated with an identifiable infectious agent, most notably dengue virus and Crimean-Congo hemorrhagic fever virus [2, 3]. As there is no single pathognomonic feature of HLS, the HLS Study Group of the Histiocyte Society established a set of diagnostic criteria [1]. A diagnosis of HLS can be made if patients have known genetic mutations related to HLS or meet ≥5 of 8 of the following clinical or laboratory criteria: (1) fever, (2) organomegaly, (3) cytopenia, (4) hypofibrinogenemia and hypertriglyceridemia, (5) hemophagocytosis, (6) loss of NK cells, (7) elevation of serum ferritin, and (8) elevated concentrations of soluble CD25 (sCD25) and soluble CD163 (sCD163) in serum [1, 4].

Ebola virus (EBOV) disease (EVD), with a reported case-fatality rate of 40%–90%, is caused by EBOV, a negative-sense single-stranded 19-kb RNA virus in the family Filoviridae [3]. Patients with EVD initially experience fever and other flulike symptoms, followed by multiple organomegaly and

Received 16 March 2023; editorial decision 30 May 2023; accepted 30 May 2023; published online 4 June 2023

[a]D. X. L. and B. P. contributed equally to this work.

[b]Present affiliation: Zoonotic and Emerging Disease Research Unit, National Bio and Agro-Defense Facility, US Department of Agriculture, Manhattan, Kansas.

Correspondence: David X. Liu, DVM, PhD, Integrated Research Facility at Fort Detrick (IRF-Frederick), Division of Clinical Research, National Institute of Allergy and Infectious Diseases, National Institutes of Health, Fort Detrick, B-8200 Research Plaza, Frederick, MD 21702 (xianhong.liu@nih.gov).

The Journal of Infectious Diseases® 2023;228:371–82

https://doi.org/10.1093/infdis/jiad203

cytopenia [5]. They also present with disseminated intravascular coagulation with low fibrinogen levels, NK cell loss, hypertriglyceridemia, and hyperferritinemia [5, 6]. EVD has been postulated as a subtype of sHLS/MAS [7]. Confirmation that EVD prompts host immune responses similar to sHLS/MAS is crucial for an early prophylactic and therapeutic protocol that may improve clinical outcomes in patients with EVD. However, limited data are available to determine the shared characteristics of sHLS/MAS and EVD because a comprehensive study of human immune responses to EBOV infection is restricted to biosafety level 4 agents [8]. In addition, the limited clinical and immunology data from human patients with EVD are confounded by the fact that samples are from patients with uncertain exposure dates and various supportive treatment regimens. Therefore, a prospective controlled natural history study using animal models is essential and critical for comparing the host immune responses between sHLS/MAS and EVD.

Nonhuman primates (NHPs) are the reference standard of animal models and have been used widely to study the pathogenesis of and treatments for EVD because they closely recapitulate most of the clinical and pathophysiologic features of human disease [5, 9, 10]. Some features of sHLS/MAS, such as fever, organomegaly, cytopenia, hypercytokinemia, and hypofibrinogenemia, have been reported in EVD models [9, 11]. However, many critical features of sHLS/MAS, such as hemophagocytosis and activation status of macrophage, T cells, NK cells, and triglyceride, have yet to be studied. Here, for the first time, we conducted a comprehensive investigation of the clinical and laboratory features of sHLS/MAS in the NHP EVD model.

METHODS

Virus, Animals, and Study Design

Detailed animal information and study design are included in Supplementary Table 1 and have been described elsewhere [12]. Briefly, 15 Chinese-origin rhesus macaques (*Macaca mulatta*) were split equally into 5 groups (3 monkeys per group) by prescheduled day of euthanasia, labeled as days 0 (uninfected control), 3, 4, 5, and 6 after exposure. Twelve other rhesus macaques were assigned to a separate terminal group (T) as exposed controls, euthanized at days 5–8 after exposure, when they reached the predetermined experimental end points of EVD. The numbers of samples used in each assay for different time points are listed in Supplementary Table 2.

All monkeys used in this study were cared for and used humanely in accordance with the following policies: the *U.S. Public Health Service Policy on Humane Care and Use of Animals* (2000); *the Guide for the Care and Use of Laboratory Animals* (2011); and the *U.S. Government Principles for the Utilization and Care of Vertebrate Animals Used in Testing, Research, and Training* (1985). The Association for Assessment and Accreditation of Laboratory Animal Care International accredits all animal facilities and programs in the National Institute of Allergy and Infectious Diseases, National Institutes of Health. This study was performed in the biosafety level 4 laboratory at the Integrated Research Facility at Fort Detrick, National Institute of Allergy and Infectious Diseases, Frederick, Maryland.

Macroscopic and Microscopic Examination

Complete postmortem examinations were performed. Tissues were collected at necropsy, fixed, and processed for histopathology and special stains [13].

Immunohistochemistry and Semiquantification of Digital Image Analysis

Immunohistochemistry for EBOV-glycoprotein, EBOV-VP40, CD163, and CD68 was performed [14]. All primary and secondary antibody information and the detailed semiquantification by digital image analysis (SQDIA) protocol are provided in Supplementary Table 3 and the Supplementary Methods, respectively.

RNAscope In Situ Hybridization

EBOV genomic RNA was detected in 4-μm sections of formalin-fixed, paraffin-embedded tissue samples analyzed with an RNAscope 2.5 HD RED kit (catalog no. 322360; Advanced Cell Diagnostics), as described elsewhere [13].

Hematology

Tripotassium ethylenediaminetetraacetic acid anticoagulated blood (Becton Dickinson) was analyzed with a Sysmex XT-2000iV (Sysmex).

Biochemistry

Serum samples were analyzed for chemistry parameters using a Piccolo general chemistry 13-panel cartridge (Abaxis).

Coagulation Assays

Frozen plasma samples were used for coagulation assay analysis using a Sysmex CS-2500.

Serum Triglycerides Quantification

Serum triglycerides in duplicates were analyzed using an EnzyChrom Triglyceride Assay Kit (BioAssay Systems), following the manufacturer's instructions. Sample triglyceride concentrations were determined from known standards after reading with a plate reader at 570 nm.

Quantification of sCD25

Total sCD25 concentrations in duplicate frozen serum samples were measured using a human CD25 ELISA kit (R&D Systems), following the manufacturer's instructions. Samples were read in a plate reader at 450 nm after subtracting the 540-nm reading values.

Quantification of sCD163

Total sCD163 concentrations from frozen serum samples in duplicates were measured using a DuoSet sandwich human CD163 ELISA kit (R&D Systems), per the manufacturer's instructions, with minor modifications. Samples were read in a plate reader at 450 nm after subtracting the 540-nm reading values.

Flow Cytometry Analysis of Whole Blood

The information on antibodies, detailed protocol, and analysis are documented in Supplementary Table 4 and the Supplementary Methods.

Cytokine/Chemokine/Growth Factor Analysis

The Invitrogen Cytokine/Chemokine/Growth Factor 37-Plex NHP ProcartaPlex Panel (Thermo Fisher Scientific) was used to measure cytokines/chemokines from frozen serum samples, according to the manufacturer's instructions. Samples were read on a Flexmap 3D reader (Luminex) within 24 hours of completion and analyzed using a 5-parameter logistic or spine curve–fitting method.

Statistical Analyses

Dunnett multiple comparisons test was used to compare the mean value at 0 days after exposure (baseline) to each time point at 1, 2, 3, 4, 5, and 6 days after exposure and at the terminal day (T). All statistical analyses and graphic presentations were performed using Prism software, version 9.1.1 (GraphPad Software). Correlation analysis between different parameters was performed with a 2-tailed Pearson correlation method. A *P* value threshold of .05 was used to assess statistical significance.

RESULTS

Hemophagocytosis is Observed in EBOV Infected Macaques

Hemophagocytosis was observed in a few spleen, lymph node, and liver macrophages but more so in the bone marrow macrophages, especially in monkeys with late-stage EVD. Morphologically, phagocytic macrophages engulfed lymphocytes, neutrophils, and/or erythrocytes in the splenic red pulp (Figure 1*A*), medullae of the lymph nodes (Figure 1*B*), bone marrow (Figure 1*C*), and hepatic Kupffer cells (Figure 1*D*), which also contained eosinophilic intracytoplasmic viral inclusion bodies.

EBOV Is Associated With the Activation of Circulating Monocytes and Resident Macrophages but Not Dendritic Cells

Serum concentrations of sCD163, a specific macrophage activation marker, increased markedly at 5 days after exposure

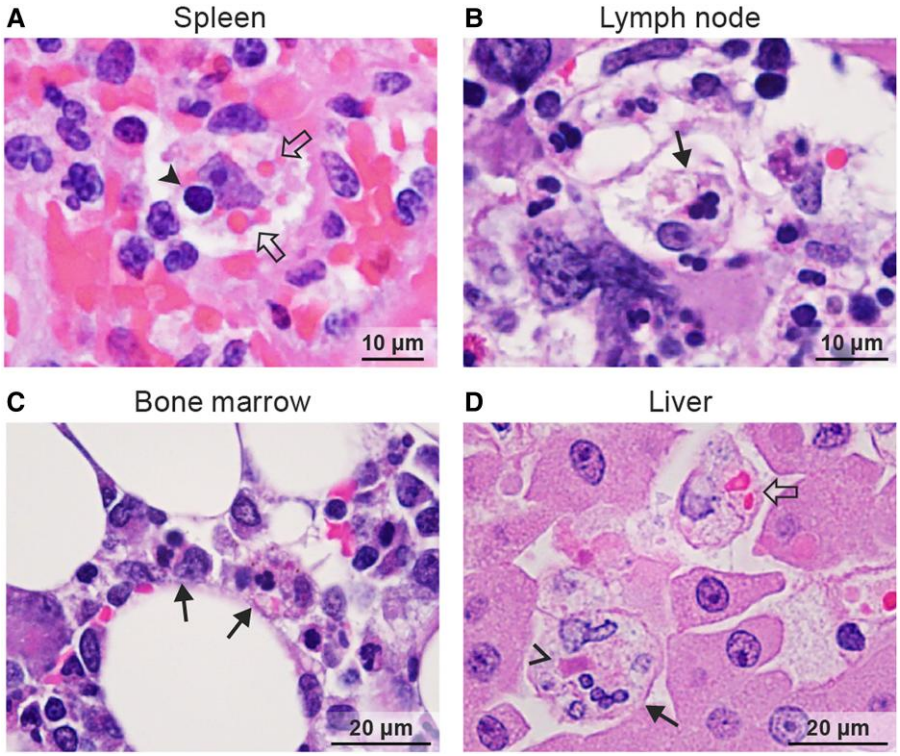

Figure 1. Hemophagocytosis in Ebola virus (EBOV)–exposed nonhuman primates (NHPs) (hematoxylin-eosin staining). Hemophagocytosis was observed in the spleen (*A*), lymph node (*B*), and bone marrow (*C*), as well as Kupffer cells in the liver (*D*) from the terminal-group control monkeys. Representative images show that macrophages phagocytize neutrophils (*arrows*), lymphocytes (*arrowhead*), and erythrocytes (empty arrows). *D,* A Kupffer cell contains an intracytoplasmic viral inclusion body (>).

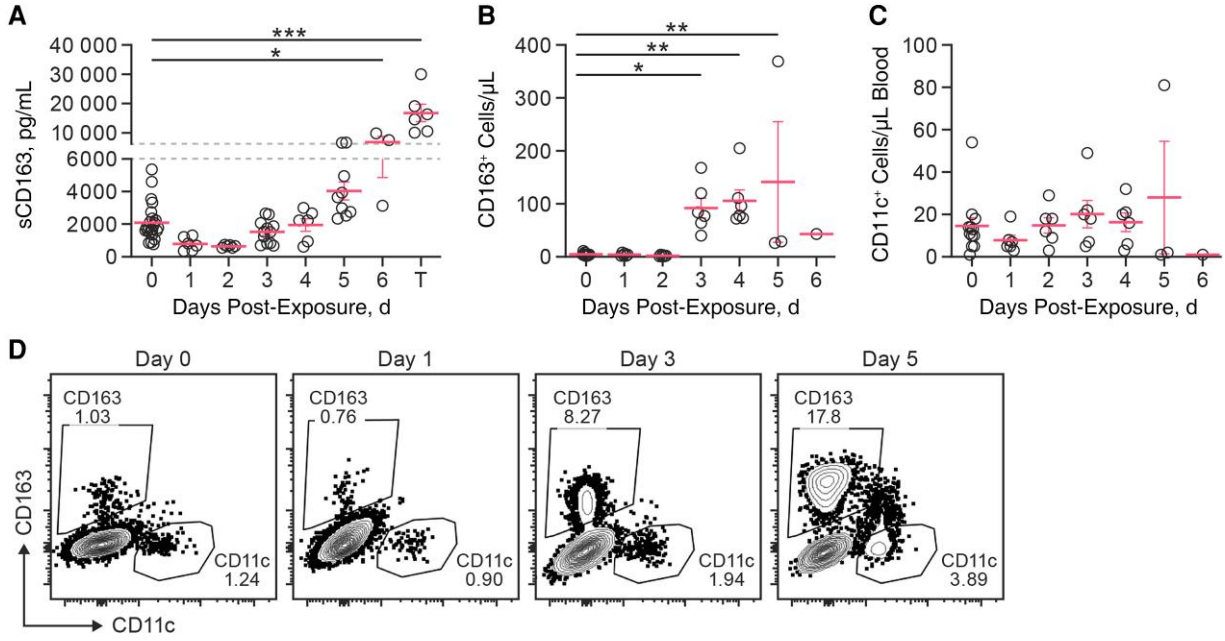

Figure 2. Serum soluble CD163 (sCD163) concentrations and circulating monocyte changes in Ebola virus (EBOV)–exposed monkeys. *A*, Significant increases in serum sCD163 concentrations at day 6 after EBOV exposure and at the terminal day (T). *B*, Flow cytometry and hematology show significant increases in total circulatory $CD3^{-}CD14^{-}CD20^{-}CD11c^{-}CD163^{+}$ cells at 3, 4, and 5 days after exposure. *C*, There were no significant differences in the $CD3^{-}CD14^{-}CD20^{-}CD163^{-}CD11c^{+}$ population during disease progression. *D*, Representative dot plots show an increased frequency of $CD163^{+}$ and $CD11c^{+}$ cells from 3 to 5 days after exposure. Each plot shows the percentage of $CD163^{+}$ and $CD11c^{+}$ cells in the gated population. $^{*}P < .05$; $^{**}P < .01$; $^{***}P < .001$.

(1.9-fold above baseline) and were significantly high at day 6 ($P = .01$) and at T ($P < .001$) (Figure 2*A*). To investigate whether increased CD163 is associated with circulating monocyte activation, the total $CD163^{+}$ cells in peripheral blood were quantified. As early as 3 days after exposure, monkeys showed a significant increase in the total $CD163^{+}$ population ($P < .04$), which remained high at 4 ($P < .005$) and 5 ($P < .003$) days after exposure, compared with baseline (Figure 2*B*). Although only a single sample from a monkey in the day 6 group was analyzed, its $CD163^{+}$ population was 10 times higher than its baseline. Analysis of peripheral monocyte-derived dendritic cells ($CD3^{-}CD14^{-}CD20^{-}CD163^{-}CD11c^{+}$) revealed no significant changes in the total peripheral $CD11c^{+}$ population during the disease course (Figures 2*C* and 2*D*). Samples were unavailable for flow cytometry in 2 of 3 monkeys in the day 6 group and all in the terminal group.

To investigate the activation status of resident tissue macrophages, we evaluated the spleen, one of the earliest EBOV-targeted organs. By immunohistochemistry, macrophage activation in the splenic white pulp differed from that in the red pulp. $CD163^{+}$ cells were undetectable in the white pulp at 0, 3, and 4 days after exposure but increased gradually at days 5 and 6. The number, size, and intensity of staining of $CD163^{+}$ macrophages increased markedly in the white pulp in all terminal-group monkeys (Figure 3*A*). SQDIA of splenic $CD163^{+}$ cells revealed that the percentage of $CD163^{+}$ cells in the white pulp increased markedly at 5 and 6 days after exposure and significantly at T ($P = .006$) (Figure 3*B*). However, the cell density in the white pulp dropped markedly at 6 days after exposure and significantly at T ($P = .008$), compared with baseline (Figure 3*C*).

$CD163^{+}$ cells in splenic red pulp were detected at 0, 3, and 4 days after exposure, but they decreased gradually from day 5 to T. SQDIA confirmed that the percentage of $CD163^{+}$ macrophages in the red pulp was reduced markedly at day 5 and significantly at day 6 ($P < .001$) and at T ($P < .001$) (Supplementary Figure 1*A*). Meanwhile, the cell density in red pulp also dropped substantially at day 6 ($P = .005$) and at T ($P < .001$) (Supplementary Figure 1*B*). In contrast, the number of $CD68^{+}$ (a pan-macrophage or M1 marker) cells was high in the white and red pulp of all monkeys, including those in the control group (Supplementary Figure 2). SQDIA showed no significant differences in $CD68^{+}$ cells between the splenic white and red pulp and during the disease progression (data not shown).

EBOV Triggers Hypercytokinemia, Correlated With Macrophage Activation

Consistent with previous NHP studies, increased levels of cytokines, compared with baseline, were detected as EVD progressed [9]. Serum interferon (IFN) γ concentrations were significantly high in terminal-group monkeys ($P < .001$).

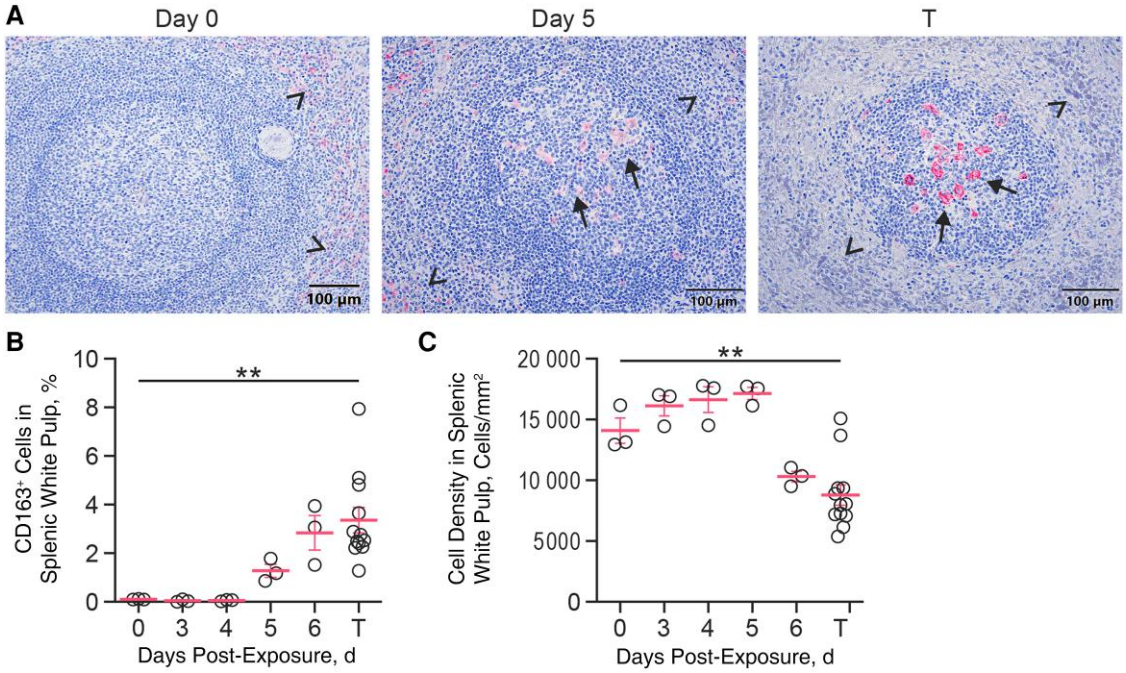

Figure 3. Immunohistochemistry (IHC) and semiquantification by digital image analysis (SQDIA) of CD163$^+$ cells in the spleen. *A*, IHC reveals that there are no (day 0; uninfected control), a small number (day 5 after exposure), and many (terminal day [T]) CD163$^+$ cells (*arrows*) in the splenic white pulp, while the number of CD163$^+$ cells in the splenic red pulp (>) decreases daily. *B, C*, SQDIA confirmed that the percentage of CD163$^+$ cells increases significantly (*B*), but cell density (*C*) is decreased significantly in the splenic white pulp at T. $^{**}P < .01$.

Serum interleukin 18 (IL-18) concentrations showed a gradual elevation from 4 to 6 days after exposure and were significantly higher at T ($P < .001$). Serum interleukin 6 (IL-6) concentrations increased sharply at day 5 and were significantly elevated at day 6 ($P = .009$) and at T ($P < .001$). Similarly, the serum interleukin 1 receptor antagonist (IL-1RA) increased slightly at 4 days after exposure and significantly at day 5 ($P < .001$), day 6 ($P < .001$), and T ($P < .001$). (Figure 4*A*) Other significantly elevated cytokines and chemokines were IFN-α, interleukin 8, macrophage inflammatory protein 1α and 1β, SDF-1α, monocyte chemoattractant protein 1, Monokine induced by gamma interferon, colony-stimulating factor 3, B lymphocyte chemoattractant, CXCL11, vascular endothelial growth factor A and D, CCL11, and stem cell factor (Supplementary Table 5). Decreased or unchanged cytokines and chemokines are listed in Supplementary Table 6.

Correlations between plasma sCD163 and major elevated cytokines were analyzed to determine whether hypercytokinemia is associated with macrophage activation. Plasma sCD163 was strongly correlated with hypercytokinemia (IFN-γ, IL-18, IL-6, and IL-1RA) (Figure 4*B*).

EBOV-Infected Rhesus Macaques Develop Significantly Elevated Serum sCD25 Concentrations, Correlated With Hypercytokinemia

T-cell activation, marked explicitly by serum CD25 levels, is observed in patients with sHLS/MAS [3]. sCD25 levels were increased markedly at 5 days after exposure (15.5 times) and were significantly higher at day 6 ($P = .02$) and at T ($P < .001$), compared with baseline (Figure 5*A*). Furthermore, correlation analysis showed that increased serum sCD25 was positively correlated with hypercytokinemia (IFN-γ, IL-18, IL-6, and IL-1RA) (Figure 5*B*).

EVD Develops Significant Hypertriglyceridemia, Correlated With Hypercytokinemia

Elevated serum triglyceride level is another diagnostic criterion of the sHLS/MAS [4]. Significant increases in serum triglyceride concentrations were observed at 6 days after exposure ($P = .007$) and at T ($P < .001$), compared with baseline (Figure 6*A*). Hypertriglyceridemia was also positively correlated with hypercytokinemia (IFN-γ, IL-18, IL-6, or IL-1RA) (Figure 6*B*).

EBOV Infection Is Associated With Reduced Activated (CD56$^+$HLA-DR$^+$) NK Cells in the Peripheral Blood

The loss of NK cells and their function are typical immune alterations in sHLS/MAS [4]. We focused on the CD3$^-$CD14$^-$CD20$^-$CD56$^+$ population that was unchanged during EVD progression other than a transient increase at 3 days after exposure (data not shown). However, when we separated the CD56$^+$ population by activation status, defined by CD56$^+$HLA-DR$^+$ populations in the CD3$^-$CD14$^-$CD20$^-$ leukocytes, the CD56$^+$HLA-DR$^+$ NK population decreased

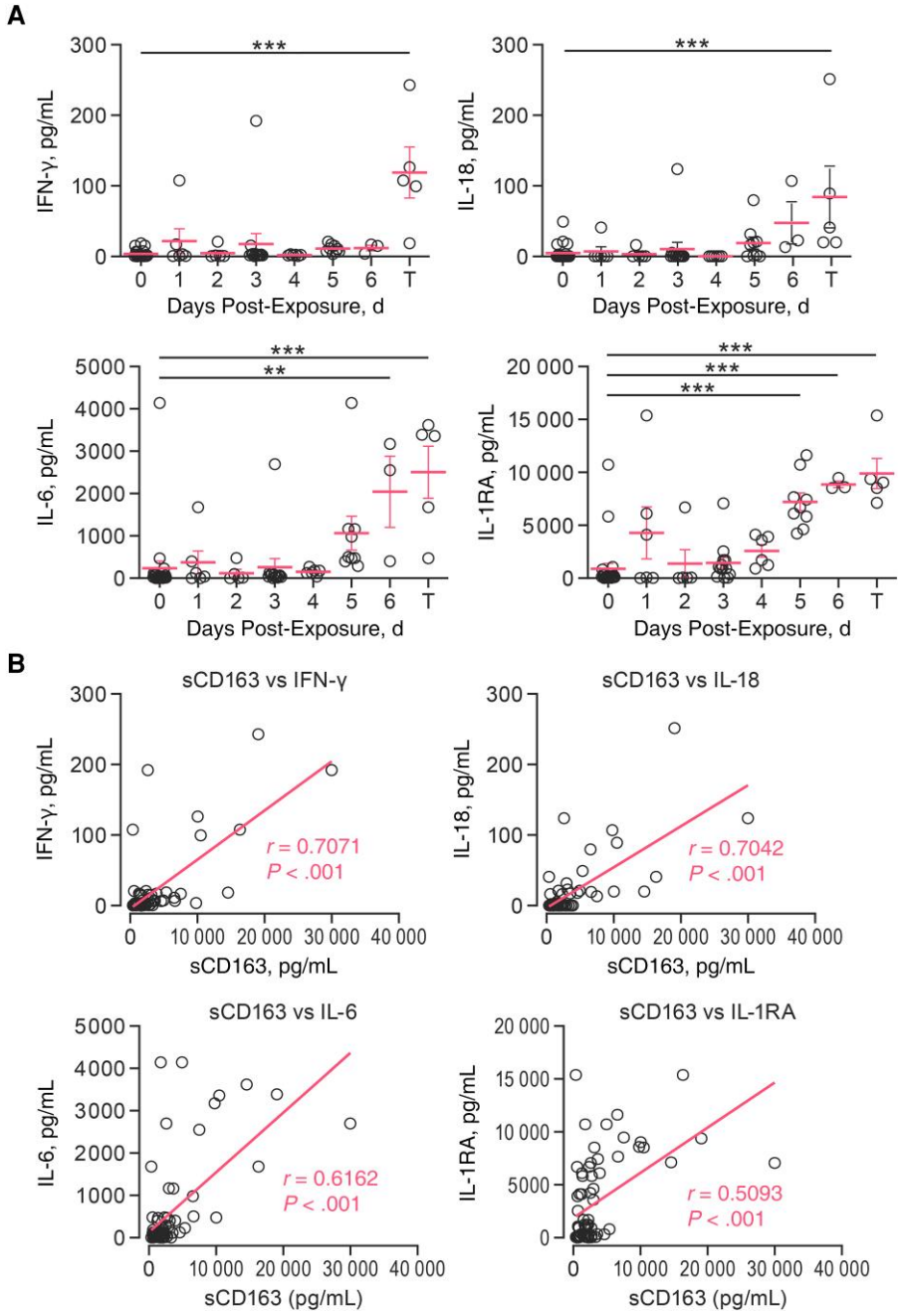

Figure 4. Serum cytokine concentrations and their correlations with soluble CD163 (sCD163). *A*, Higher serum concentrations of interferon (IFN) γ and interleukin 18, 6, and 1RA (IL-18, IL-6, and IL-1RA) were detected during disease progression. *B*, Significant positive correlations between sCD163 and IFN-γ, IL-18, IL-6, or IL-1RA. Data were analyzed by means of simple linear regression analysis. $^{**}P < .01$; $^{***}P < .001$.

significantly as early as 1 ($P = .03$) and 2 days after exposure ($P = .002$), compared with baseline, although a transient increase in the $CD56^{+}HLA\text{-}DR^{+}$ NK population was noticed at day 3 ($P = .02$). However, they dropped sharply again at day 4 ($P = .03$), compared with the baseline, and remained at lower levels (66.7% and 3.6% of baseline at days 5 and 6, respectively) (Figure 7*A*). In contrast, the $CD56^{+}HLA\text{-}DR^{-}$ NK population remained unchanged throughout the study period, except for a transient significant increase at day 4 ($P = .02$), compared with baseline (Figure 7*B* and 7*C*). Unfortunately, owing to the sample volume limitations, we could not measure the $CD56^{+}$ NK population at T time points.

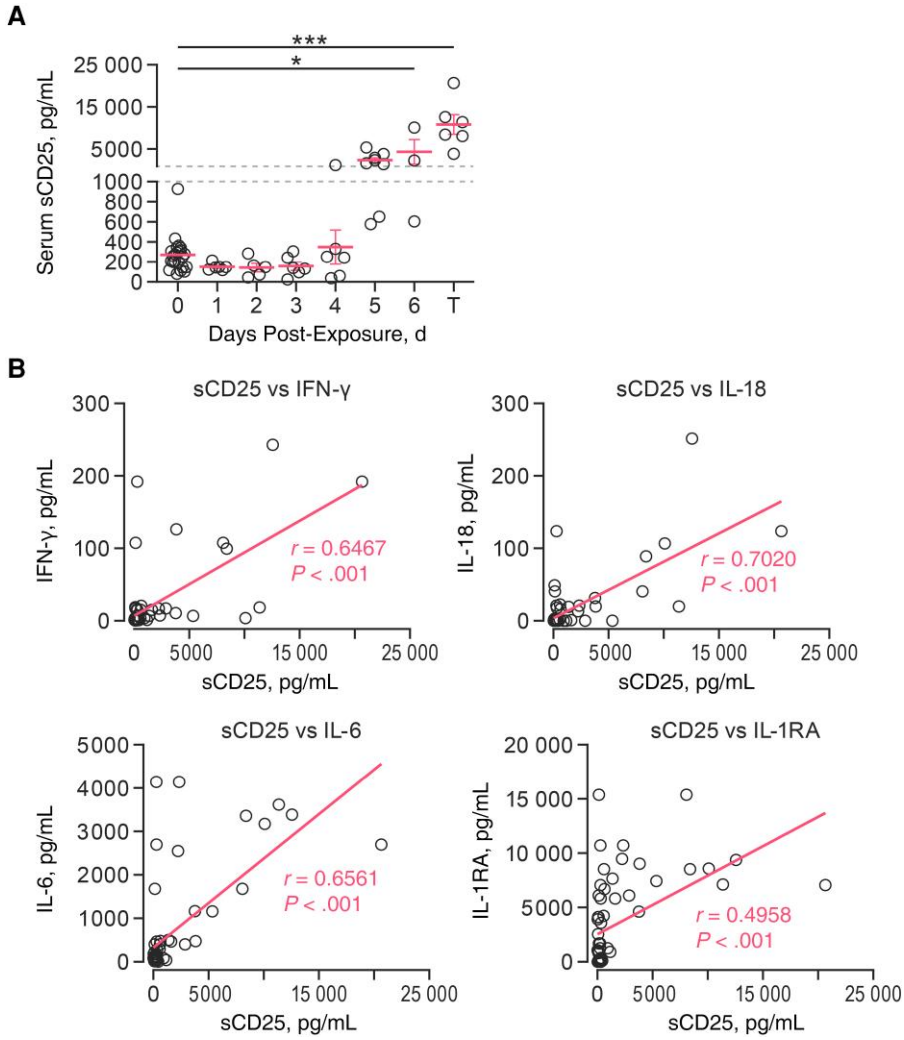

Figure 5. Serum soluble CD25 (sCD25) concentrations and their positive correlations with cytokines. *A*, Higher serum concentrations of sCD25 at day 6 after exposure and at the terminal day (T). *B*, sCD25 concentrations were correlated positively with interferon (IFN) γ and interleukin 18, 6, and 1RA (IL-18, IL-6, and IL-1RA). $^{*}P < .05$; $^{***}P < .001$.

Positive Correlations Among Serum sCD163, sCD25, and Triglyceride Concentrations, Which Are Also Positively Correlated With Plasma Viral Load During EVD Progression

To determine whether macrophage activation, T-cell activation, and hypertriglyceridemia are correlated during EVD progression, time point–matched data for each monkey were analyzed by simple linear regression. High positive correlations were determined between sCD163 and sCD25, sCD163 and triglycerides, and sCD25 and triglycerides (Supplementary Figure 3). Furthermore, we determined whether plasma viral load (PVL) [11] is correlated with macrophage activation, T-cell activation, hypertriglyceridemia, and hypercytokinemia. Positive correlations were observed between PVL and the following: sCD163, sCD25, triglyceride, IFN-γ, IL-18, IL-6, and IL-1RA (Supplementary Figure 4).

EBOV-Infected Rhesus Macaques Share Common Clinical and Laboratory Features With sHLS/MAS Diagnostic Criteria

Consistent with previous reports [9, 11], clinical and laboratory findings typical of sHLS/MAS were observed in this study (Supplementary Results). Clinically, fever was one of the earliest clinical signs observed in monkeys with EVD (Supplementary Figure 5*A*). Splenomegaly, hepatomegaly, and peripheral lymphadenopathy were the marked pathologic lesions at necropsy (Supplementary Figure 5*B*). Typical histopathologic lesions consistent with EVD were observed, and immunohistochemistry and/or in situ hybridization confirmed EBOV antigen and/or genomic RNA in all of these organs (Supplementary Figure 6). Pancytopenia (Supplementary Figure 7), hypofibrinogenemia, and disseminated intravascular coagulation developed during EVD progression, especially in late-stage EVD (Supplementary Figure 8).

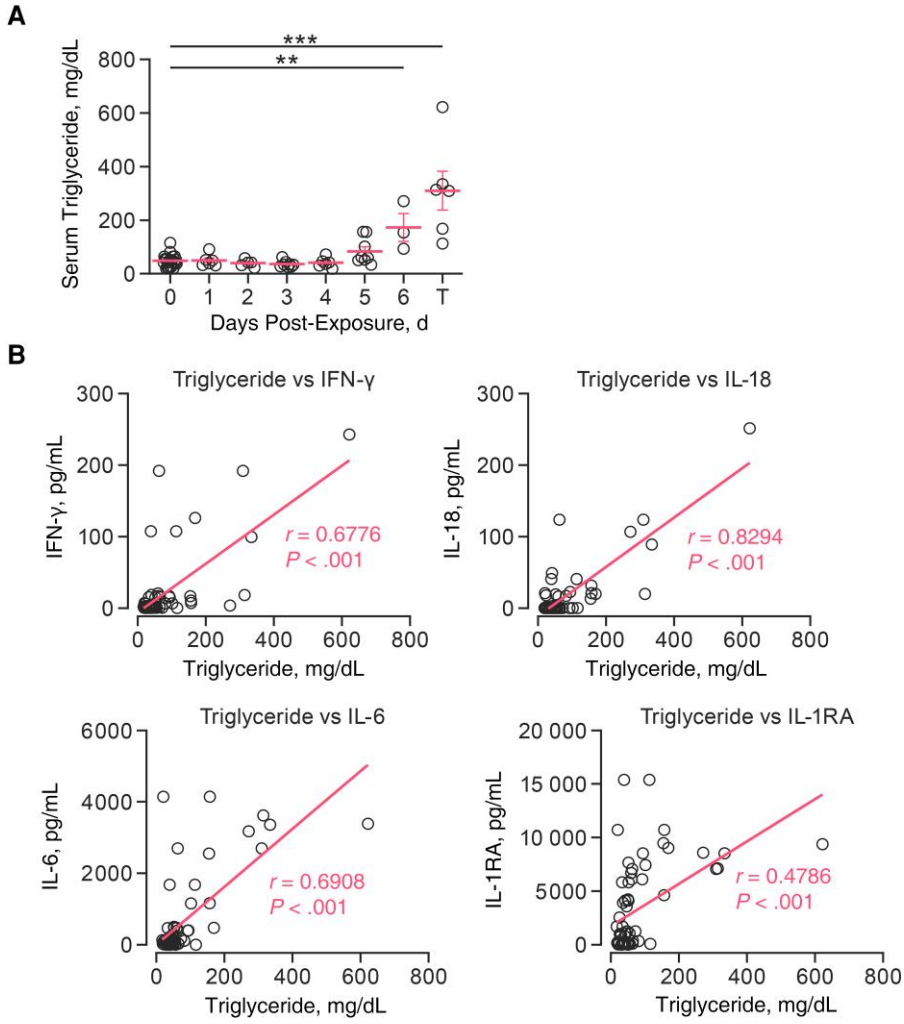

Figure 6. Serum triglyceride concentrations and their positive correlation with cytokines. *A*, Higher serum triglyceride concentrations at day 6 after exposure and at the terminal day (T). *B*. Positive correlations were detected between triglycerides and interferon (IFN) γ and interleukin 18, 6, and 1RA (IL-18, IL-6, or IL-1RA). $^{**}P < .01$; $^{***}P < .001$.

DISCUSSION

To our knowledge, this is the first detailed systemic characterization of the known features of sHLS/MAS in a lethal NHP model of EVD. Clinical, pathologic, and immunologic findings in lethally EBOV-infected monkeys have striking similarities to findings in sHLS/MAS [1, 4].

Macrophage activation, characterized by an increased serum level of sCD163, is a significant laboratory feature in sHLS/MAS. This has been reported retrospectively in small numbers of patients with EVD and patients with Sudan virus disease (SVD); notably, in both populations, levels of sCD163 were associated with severity or fatal disease [1, 3, 4]. In the current study, sCD163 is associated with up-regulated expression of CD163 on circulating and tissue macrophages. A high correlation of plasma sCD163 and PVL confirms that EBOV not only infects but also activates both circulating monocytes and tissue macrophages. Again, the high positive correlation between sCD163 and hypercytokinemia suggests that macrophage activation plays a central role in orchestrating the excessive inflammation seen in patients with EVD. In addition, the lack of changes in monocyte-derived dendritic cells in the current study implies that these cells are not the foremost player involved in immune responses during the EVD progression, although EBOV can infect monocyte-derived dendritic cells in vitro [15].

T-cell activation, characterized by significant elevation of sCD25, is another typical feature of the dysregulated immune response in the sHLS/MAS [1]. Increased sCD25 was also described in a small number of patients with EVD and larger numbers of patients with SVD [3]; however, as opposed to sCD163, sCD25 was not discriminatory for severe and/or fatal disease [3]. The progressive increase in sCD25 concentrations, especially at the end stage, is newly characterized here.

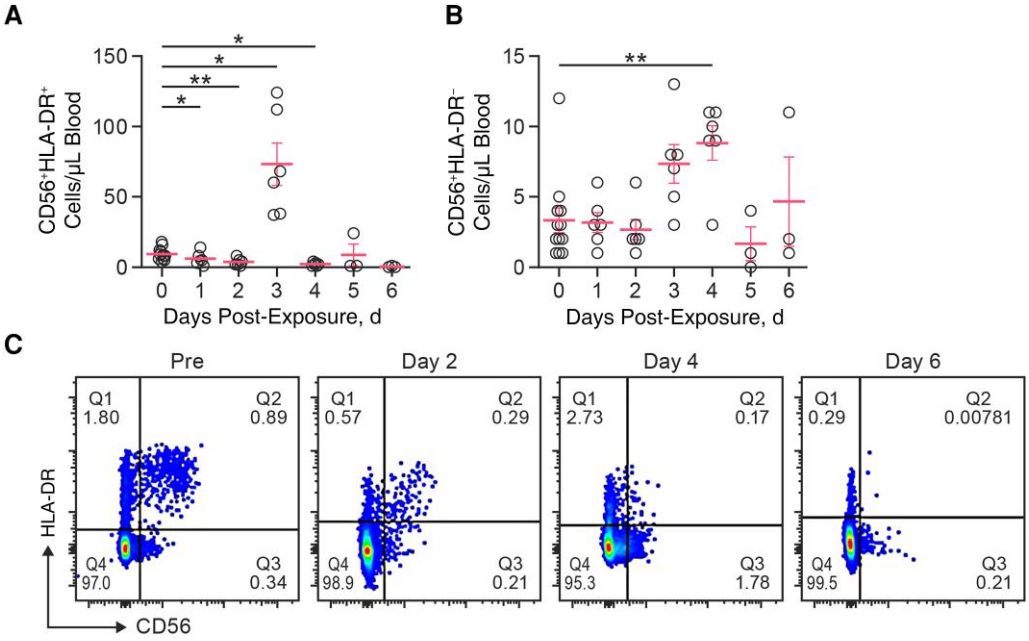

Figure 7. Effect of Ebola virus (EBOV) infection on CD56$^+$ peripheral natural killer (NK) cells in rhesus monkeys. *A.* The CD56$^+$HLA-DR$^+$–activated NK population decreased significantly at 1, 2, and 4 days after exposure, except for a transient increase observed at day 3. *B.* The CD56$^+$HLA-DR$^-$–activated NK population remained steady throughout the study but was higher at day 4. *C.* Representative CD56 and HLA-DR phenotypic expressions are seen in whole-blood samples from an EBOV-exposed monkey. Note that CD56$^+$HLA-DR$^+$ cells started decreasing on day 2 and remained low throughout the study. $^*P < .05$; $^{**}P < .01$. Q1, HLA-DR+CD56-; Q2, HLA-DR+CD56+; Q3, HLA-DR-CD56+; Q4, HLA-DR-CD56-.

Furthermore, the high positive correlation between sCD25 and hypercytokinemia confirms prior reports that T-cell activation also plays a significant role in the host immune response to EBOV infection. Although the mechanism of T-cell activation is unclear, the T-cell immunoglobulin and mucin domain 1 (TIM-1)$^{-/-}$ and wild-type mouse models suggest that mouse-adapted EBOV can activate T lymphocytes by binding directly to Tim-1 and inducing increased cytokine production [16].

A decrease in NK cells has been observed in fatal outcomes in cynomolgus macaques with EVD [17] or in humans with sHLS/MAS [1]. In the current study, we did not observe a significant loss in the total NK cell population, likely owing to insufficient samples from monkeys with end-stage EVD. However, early loss (by 1 day after exposure) of activated (CD56$^+$HLA-DR$^+$) NK cells is likely due to the lack of early activation of IFN-γ and/or IL-18 [18]. The lack of early NK-mediated innate function in EBOV-exposed monkeys may result in prolonged innate and adaptive immune-cell interactions and excessive up-regulation of inflammatory cytokine up-regulations, including IFN-γ, IL-6, and IL-18, as reported for sHLS/MAS [19].

Hemophagocytosis is typically observed in the spleen, peripheral lymph nodes, bone marrow, and liver in patients with sHLS/MAS. We demonstrated that activated macrophages can engulf blood cells, including red blood cells, lymphocytes, and neutrophils, during EVD. Hemophagocytosis appears to be a typical response to sustained or severe inflammation with a high IFN-γ, sCD25, and/or sCD163 [19]. In addition, EBOV-exposed monkeys, especially at terminal stages of the disease, develop hypertriglyceridemia, 1 of 8 diagnostic criteria for HLS [20]. Hypertriglyceridemia discriminated between fatal and nonfatal disease in SVD [3]. Furthermore, the positive correlations between hypertriglyceridemia and hypercytokinemia, sCD163, sCD25, and PVL suggest that hypertriglyceridemia is associated with high levels of tumor necrosis factor α and IFN-γ, leading to decreased activity of lipoprotein lipase and a hepatic source [4].

Consistent with findings of many previous studies [8, 9, 21], fever, organomegaly, pancytopenia, hyperferritinemia with disseminated intravascular coagulation, and hypercytokinemia are the most common clinical and laboratory findings in both sHLS/MAS and EVD [1, 3]. Hypercytokinemia plays an essential role in the pathogenesis of the sHLS/MAS [22, 23]. Excessive but ineffective inflammation and marked hypercytokinemia is a crucial feature of sHLS/MAS [22, 23], consistent with our findings and prior reports in NHPs and human EVD. Particular cytokine elevations may suggest interventional opportunities. IL-6, a proinflammatory cytokine, has been closely associated with fever, anemia, T-lymphocyte activation, and the suppression of NK cell activity during sHLS/MAS.

A significantly elevated serum IL-1RA levels in EBOV-exposed monkeys at 5 days after exposure onward also agrees with a previous report in which patients with EVD with fatal outcomes had increased IL-1RA levels [24]. NHPs in the current study had EBOV exposure–associated alterations in other cytokines, with slight variables compared with those in previous reports [25, 26]. Regardless, the inflammation characteristic of sHLS/MAS appears not to be dependent on any single cytokine; instead, a complex set of cytokines and chemokines reflect unchecked activation and proliferation of monocytes/macrophages and lymphocytes [23, 27].

Hyperferritinemia is likely associated with ferritin accumulation during the anti-inflammatory process of macrophage scavenging of heme via the CD163 receptor [4]. It is associated with fatal outcomes in patients with SVD and is believed to be a sensitive and specific predictor of sHLS/MAS [3, 20]. However, we could not measure ferritin levels owing to the lack of cross-reactivity of commercially available kits with NHP serum samples.

In conclusion, EBOV-infected rhesus macaques are characterized by fever, organomegaly, cytopenia, hypofibrinogenemia and hypertriglyceridemia, hemophagocytosis, loss of activated NK cells, and elevated sCD25 and sCD163 levels in serum, meeting 7 of 8 clinical or laboratory criteria for diagnosing sHLS/MAS. It should be acknowledged that a shared disease "phenotype" may be just that, and whether or not these commonalities reflect an underlying "endotype" remains to be determined [28]. Nonetheless, the striking similarities advocate for exploration of common mechanisms of disease, particularly in the subset of patients with EVD with multisystem organ dysfunction and obvious immunopathology. When possible, existing human EVD data sets could be retrospectively mined to determine whether, for example, serum ferritin and sCD163 are prognostically helpful to identify a subset of severely ill patients with EVD who might benefit from targeted immunomodulation in addition to approved monoclonal antibody–based therapies.

Current strategies (or strategies under clinical study) for sHLS/MAS might inform the preclinical or clinical evaluation of novel immunomodulatory approaches to supplement EBOV-specific approved therapies. First-line "shotgun" therapies for sHLS/MAS (eg, a combination of etoposide and dexamethasone) are unlikely to be tolerated in patients with EVD and may cause harm. However, if a shared endotype exists, tailored "scalpels," that is, immunomodulatory opportunities to target host immunopathology, merit consideration for preclinical evaluation in EVD, albeit with *primum non nocere* caution. Several potential treatments for sHLS/MAS are being studied, including emapalumab (an anti-IFN-γ antibody) [26, 27, 29] ruxolitinib (a Janus kinase 1 inhibitor that targets IL-6 and IFN-γ signals provided 73% complete remission in pediatric patients with sHLS/MAS) [30], tocilizumab (target IL-6) [31], and anakinra (recombinant IL-1RA) [32], among others.

Supplementary Data

Supplementary materials are available at *The Journal of Infectious Diseases* online. Consisting of data provided by the authors to benefit the reader, the posted materials are not copy-edited and are the sole responsibility of the authors, so questions or comments should be addressed to the corresponding author.

Notes

Acknowledgments. We thank Danny Ragland, Peter Jahrling, Bobbi Barr, Anthony Marketon, Nejra Isic, and John Bernbaum for their support and technical assistance and Anya Crane for technical writing services.

Author contributions. D. X. L. conceptualized the study. D. X. L., B. P., and H. X. designed the study and analyzed the data. D. X. L., B. P., T. K. C., D. L. P., L. M. H., R. D. A., A. M. W. H., R. J. H., R. Bernbaum, D. R., S. A., R. Byrum, K. C., R. R., J. K., and K. H. performed experiments and data collection. D. X. L. and B. P. wrote the original draft. T. K. C., D. P. L., R. B., K. C., M. R. H., and L. E. H. reviewed and edited the manuscript. J. W. prepared the graphical abstract and figures. M. S. C., I. C., G. W., R. S. B., T. W., M. R. H., C. S. S., and L. E. H. performed project administration.

Disclaimer. The views and conclusions contained in this document are those of the authors and should not be interpreted as necessarily representing the official policies, either expressed or implied, of the US Department of Health and Human Services or of the institutions and companies affiliated with the authors, nor does mention of trade names, commercial products, or organizations imply endorsement by the US government.

Financial support. This work was supported by the National Institute of Allergy and Infectious Diseases (prime contract with Battelle Memorial Institute [HHSN272200700016I] and subsequently with Laulima Government Solutions [HHSN272201800013C] and by the National Cancer Institute (contract 75N910D00024 with Leidos Biomedical Research), National Institutes of Health. D. X. L., B. P., T. K. C., D. L. P., L. M. H., R. D. A., R. J. H., R. Bernbaum, D. R., S. A., R. Byrum, K. C., R. R., J. K., K. H., J. W., G. W., R. S. B., T. W., and M. R. H. performed this work as employees of Laulima Government Solutions. A. M. W. H. performed this work as an employee of Tunnell Government Services, a subcontractor to Laulima Government Solutions. I. C. performed this work as an employee of Leidos Biomedical Research, as supported by the Clinical Monitoring Research Program Directorate, Frederick National Laboratory for Cancer Research, sponsored by the National Cancer Institute.

Potential conflicts of interest. All authors: No reported conflicts.

All authors have submitted the ICMJE Form for Disclosure of Potential Conflicts of Interest. Conflicts that the editors

consider relevant to the content of the manuscript have been disclosed.

References

1. Al-Samkari H, Berliner N. Hemophagocytic lymphohistiocytosis. Annu Rev Pathol **2018**; 13:27–49.
2. Tan LH, Lum LC, Omar SF, Kan FK. Hemophagocytosis in dengue: comprehensive report of six cases. J Clin Virol **2012**; 55:79–82.
3. McElroy AK, Shrivastava-Ranjan P, Harmon JR, et al. Macrophage activation marker soluble CD163 associated with fatal and severe Ebola virus disease in humans. Emerg Infect Dis **2019**; 25:290–8.
4. George MR. Hemophagocytic lymphohistiocytosis: review of etiologies and management. J Blood Med **2014**; 5:69–86.
5. Baseler L, Chertow DS, Johnson KM, Feldmann H, Morens DM. The pathogenesis of Ebola virus disease. Annu Rev Pathol **2017**; 12:387–418.
6. McElroy AK, Erickson BR, Flietstra TD, et al. Ebola hemorrhagic fever: novel biomarker correlates of clinical outcome. J Infect Dis **2014**; 210:558–66.
7. Van der Ven AJ, Netea MG, van der Meer JW, de Mast Q. Ebola virus disease has features of hemophagocytic lymphohistiocytosis syndrome. Front Med (Lausanne) **2015**; 2:4.
8. McElroy AK, Akondy RS, McLlwain DR, et al. Immunologic timeline of Ebola virus disease and recovery in humans. JCI Insight **2020**; 5:e137260.
9. Geisbert TW, Hensley LE, Larsen T, et al. Pathogenesis of Ebola hemorrhagic fever in cynomolgus macaques: evidence that dendritic cells are early and sustained targets of infection. Am J Pathol **2003**; 163:2347–70.
10. Baskerville A, Bowen ET, Platt GS, McArdell LB, Simpson DI. The pathology of experimental Ebola virus infection in monkeys. J Pathol **1978**; 125:131–8.
11. Twenhafel NA, Mattix ME, Johnson JC, et al. Pathology of experimental aerosol *Zaire ebolavirus* infection in rhesus macaques. Vet Pathol **2013**; 50:514–29.
12. Bennett RS, Logue J, Liu DX, et al. Kikwit Ebola virus disease progression in the rhesus monkey animal model. Viruses **2020**; 12:753.
13. Liu DX, Cooper TK, Perry DL, et al. Expanded histopathology and tropism of Ebola virus in the rhesus macaque model: potential for sexual transmission, altered adrenomedullary hormone production, and early viral replication in liver. Am J Pathol **2022**; 192:121–9.
14. Liu DX, Perry DL, Cooper TK, et al. Peripheral neuronopathy associated with Ebola virus infection in rhesus macaques: a possible cause of neurological signs and symptoms in human Ebola patients. J Infect Dis **2020**; 222: 1745–55.
15. Gupta M, Mahanty S, Ahmed R, Rollin PE. Monocyte-derived human macrophages and peripheral blood mononuclear cells infected with Ebola virus secrete MIP-1α and TNF-α and inhibit poly-IC-induced IFN-α in vitro. Virology **2001**; 284:20–5.
16. Younan P, Iampietro M, Nishida A, et al. Ebola virus binding to tim-1 on T lymphocytes induces a cytokine storm. mBio **2017**; 8:e00845-17.
17. Reed DS, Hensley LE, Geisbert JB, Jahrling PB, Geisbert TW. Depletion of peripheral blood T lymphocytes and NK cells during the course of Ebola hemorrhagic fever in cynomolgus macaques. Viral Immunol **2004**; 17:390–400.
18. Horowitz A, Stegmann KA, Riley EM. Activation of natural killer cells during microbial infections. Front Immunol **2012**; 2:88.
19. Crayne CB, Albeituni S, Nichols KE, Cron RQ. The immunology of macrophage activation syndrome. Front Immunol **2019**; 10:119.
20. Campo M, Berliner N. Hemophagocytic lymphohistiocytosis in adults. Hematol Oncol Clin North Am **2015**; 29:915–25.
21. Zapata JC, Cox D, Salvato MS. The role of platelets in the pathogenesis of viral hemorrhagic fevers. PloS Negl Trop Dis **2014**; 8:e2858.
22. Mazodier K, Marin V, Novick D, et al. Severe imbalance of IL-18/IL-18BP in patients with secondary hemophagocytic syndrome. Blood **2005**; 106:3483–9.
23. Brisse E, Wouters CH, Matthys P. Hemophagocytic lymphohistiocytosis (HLH): a heterogeneous spectrum of cytokine-driven immune disorders. Cytokine Growth Factor Rev **2015**; 26:263–80.
24. Baize S, Leroy EM, Georges AJ, et al. Inflammatory responses in Ebola virus-infected patients. Clin Exp Immunol **2002**; 128:163–8.
25. Hensley LE, Young HA, Jahrling PB, Geisbert TW. Proinflammatory response during Ebola virus infection of primate models: possible involvement of the tumor necrosis factor receptor superfamily. Immunol Lett **2002**; 80:169–79.
26. Ebihara H, Rockx B, Marzi A, et al. Host response dynamics following lethal infection of rhesus macaques with *Zaire ebolavirus*. J Infect Dis **2011**; 204(suppl 3):S991–9.
27. Canna SW, Wrobel J, Chu N, Kreiger PA, Paessler M, Behrens EM. Interferon-gamma mediates anemia but is dispensable for fulminant Toll-like receptor 9-induced macrophage activation syndrome and hemophagocytosis in mice. Arthritis Rheum **2013**; 65:1764–75.
28. Reddy K, Sinha P, O'Kane CM, Gordon AC, Calfee CS, McAuley DF. Subphenotypes in critical care: translation into clinical practice. Lancet Respir Med **2020**; 8:631–43.
29. De Benedetti F, Grom AA, Brogan PA, et al. Efficacy and safety of emapalumab in macrophage activation syndrome. Ann Rheum Dis **2023**; 82:857–65.

30. Zhang Q, Zhao YZ, Ma HH, et al. A study of ruxolitinib response-based stratified treatment for pediatric hemophagocytic lymphohistiocytosis. Blood **2022**; 139: 3493–504.
31. Yamabe T, Ohmura SI, Uehara K, Naniwa T. Macrophage activation syndrome in patients with adult-onset Still's disease under tocilizumab treatment: a single-center observational study. Mod Rheumatol **2022**; 32:169–76.
32. Phadke O, Rouster-Stevens K, Giannopoulos H, Chandrakasan S, Prahalad S. Intravenous administration of anakinra in children with macrophage activation syndrome. Pediatr Rheumatol Online J **2021**; 19:98.